applied sciences

MDPI

Article

Circadian and Tidal Changes in Snapping Shrimp (*Alpheus brevicristatus*) Sound Observed by a Moored Hydrophone in the Coastal Sea of Western Jeju

Inyong Jeong and Dong-Guk Paeng *

Department of Ocean System Engineering, Jeju National University, 102 Jejudaehak-ro, Jeju-si 63243, Jeju Special Self-Governing Province, Korea; iyjeong@office.jejunu.ac.kr
* Correspondence: paeng@jejunu.ac.kr

Abstract: Numerous studies have evaluated the acoustic characteristics of soniferous snapping shrimp, but a few are based on long-term mooring measurements. In this study, underwater ambient noise signals were collected from a hydrophone moored 10 m from the sea bed in the coastal sea of western Jeju, South Korea, from mid-September 2019 for 90 days to analyze the variation in the sound of snapping shrimp. The kernel signal and a threshold value were utilized to identify the snapping shrimp, and the snap rate per minute was computed for quantitative analysis. The results show that the mean and standard deviation of the snap rate in the western sea of Jeju was 2132 ± 432 per minute during the whole measurement period. The surface water temperature and tidal level decreased by 7 °C from 25 °C and 50 cm from 190 cm, respectively, over 90 days. The snap rate decreased from September mainly due to the decrease in water temperature by 71 times per minute for every 1 °C decrease. It showed a circadian cycle, increasing by 17~24% at sunrise and sunset compared to the daytime minimum. The snap rate at night was the highest in late summer but the rate dropped like the one during the day in late fall. The snap rate at high tide was 13% higher on average than at low tide. The circadian and tidal changes of the snapping shrimp sound from long-term mooring measurements may be used as primary data for underwater ambient noise and the ecological behavior of snapping shrimp.

Keywords: snapping shrimp; snap rate; underwater ambient noise; Jeju coastal sea; circadian cycle; tidal cycle

check for updates

Citation: Jeong, I.; Paeng, D.-G. Circadian and Tidal Changes in Snapping Shrimp (*Alpheus brevicristatus*) Sound Observed by a Moored Hydrophone in the Coastal Sea of Western Jeju. *Appl. Sci.* **2022**, *12*, 6493. https://doi.org/10.3390/app12136493

Academic Editor: Alexander Sutin

Received: 6 May 2022
Accepted: 23 June 2022
Published: 27 June 2022

Publisher's Note: MDPI stays neutral with regard to jurisdictional claims in published maps and institutional affiliations.

Copyright: © 2022 by the authors. Licensee MDPI, Basel, Switzerland. This article is an open access article distributed under the terms and conditions of the Creative Commons Attribution (CC BY) license (https://creativecommons.org/licenses/by/4.0/).

1. Introduction

Various acoustic sources generate underwater noise in the ocean, and the noise level and frequency differ depending on the sources, such as ocean current and turbulence, wind, rainfall, aquatic organisms, and ships [1,2]. The ambient noise in shallow water is more complex. Still, it can be divided into two categories, one from human activities and the other from natural phenomena, which have different frequency characteristics [1,2]. Ship noise affects frequencies below 100 Hz but sometimes up to 1 kHz [3–7]. The natural noise generated by waves, aquatic life, and thermal and aquatic biological noise affect the high-frequency band above 1 kHz [8–11].

The soundscape study in the habitats of snapping shrimp revealed that snapping is the dominant noise source in the high-frequency band in the coral reefs [12–14]. As a result of studying the diurnal variation of underwater ambient noises in the habitats of the snapping shrimp in the west and south seas of Korea, it was observed that the activity of snapping shrimp showed more dependence on the water temperature rather than the wind speed and the twilight [15]. The soundscape trend measured at various locations at the estuary showed semidiurnal tide characteristics [12,16,17]. Still, there was no noticeable change in shrimp sound with tidal and lunar phases, unlike other previous investigations [12,18,19]. Our earlier study confirmed that the sound in the low-frequency band (~100 Hz) changes

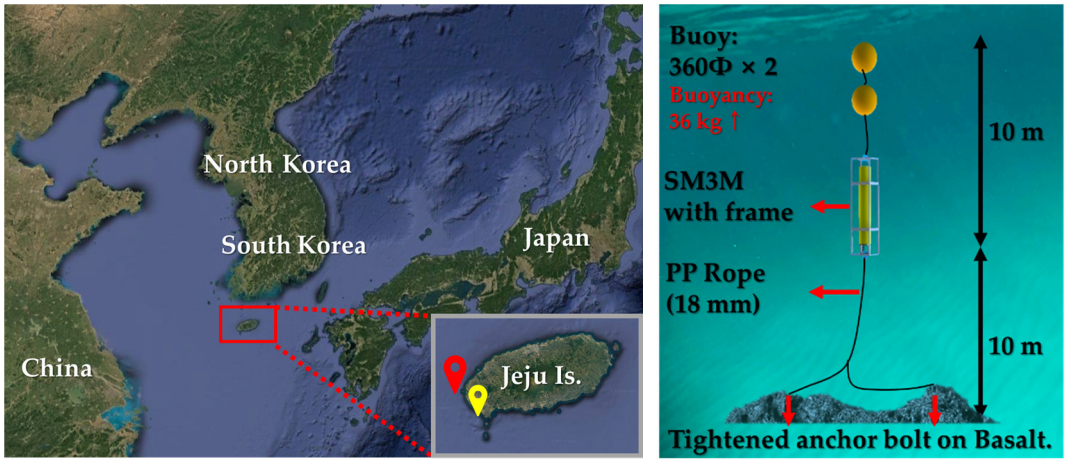
with the tide and the lunar cycle [20]. To observe the circadian and tidal characteristics of snapping shrimp sounds, it is necessary to measure the sound for an extended period.

In this paper, underwater ambient noise was measured by a moored hydrophone for 3 months to investigate the temporal change of the sound of snapping shrimp near the wave power generation test site in the western part of Jeju Island, South Korea. Snap rate per minute was computed and analyzed based on the acquired acoustic data showing circadian and tidal variations.

2. Materials and Methods

2.1. Field Recordings of Acoustic Data

The acoustic signals were measured in the waters of Hangyeong-myeon (33°19′48.9″ N 126°08′59.7″ E, Red symbol, shown in Figure 1) in the western part of Jeju Island, South Korea, from 11 September to 15 December 2019. A total of 36,000 min of data was collected by an omnidirectional hydrophone twice for 45 consecutive days (10 min per hour) at a sampling rate of 96 kHz. The hydrophone (SM3M, Wildlife Acoustics Inc., Maynard, MA, USA) was fixed to a basalt rock and placed 10 m above the floor at a bottom depth of 20 m, as illustrated in Figure 1. The Moseulpo tidal station provided the surface water temperature and tidal level (33°12′50.8″ N 126°15′04.5″ E, Yellow mark, shown in Figure 1), and the observation period was measured once every 10 min. Tidal level and surface water temperature were expressed as median values for 1 h according to the interval between sound samples.



(**a**) (**b**)

Figure 1. (**a**) The location of the hydrophone installation. The Hankyung-myeon area in the western region of Jeju Island (Red mark: 33°19′48.9″ N 126°08′59.7″ E) and Moseulpo tidal station (Yellow mark: 33°12′50.8″ N 126°15′04.5″ E); (**b**) Schematic diagram of the installation of a hydrophone (SM3M, Wildlife Acoustics Inc.) at a depth of 10 m from the seabed.

2.2. Snap Detection and Analysis

The snapping shrimp sound waveforms are impulse signals and exhibit broadband frequency characteristics [21–26]. There are many impulsive models such as Class B and alpha noise to extract impulse signals underwater [27,28]. However, this study extracted signals in the same way as in Figure 2 to compare with other studies that calculated snap rates similarly. To minimize ship noise from the total 10 min data, the smallest mean power spectrum (mean PS) value between 100 and 1500 Hz was extracted and further processed, bypassing the main frequency band (1.5~20 kHz) of the snapping shrimp sound signal [16,17,20,29].

$$S(t) = \frac{\sum \epsilon(t)\kappa(t)}{\sqrt{\sum \epsilon(t)^2 \kappa(t)^2}} \quad (1)$$

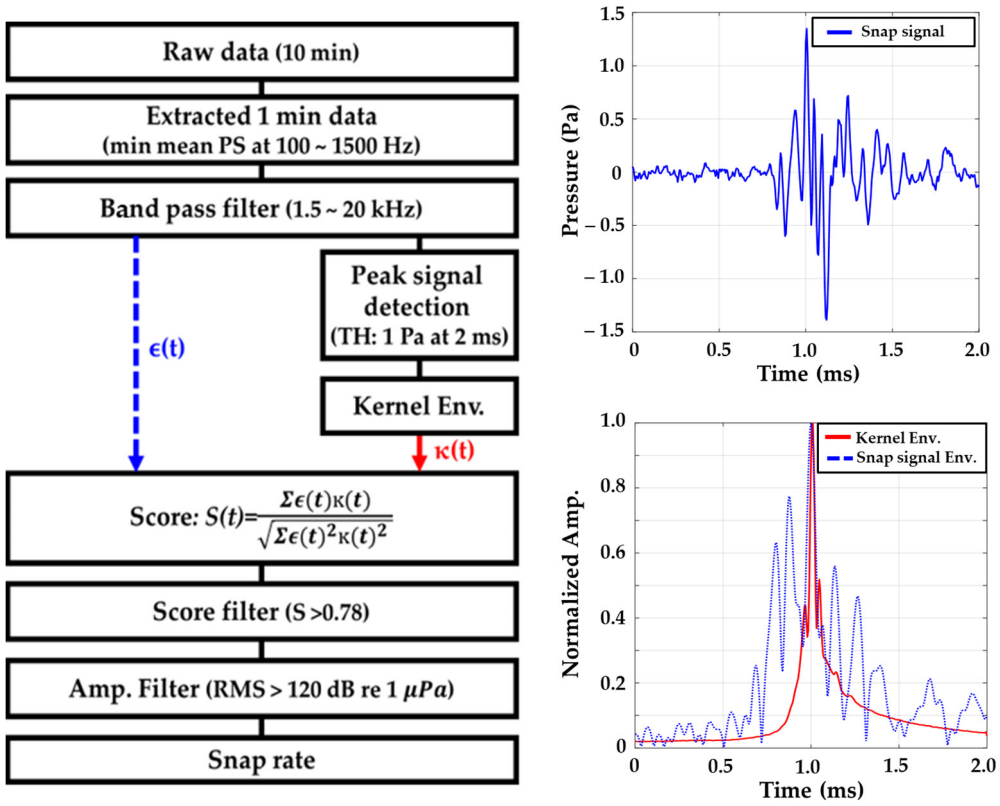


Figure 2. The snapping shrimp signal detection method. (**a**) Flow chart of the snapping shrimp signal detection. (**b**) Snapping shrimp sound and the kernel function for score calculation (Blue line: snap signal; blue dotted line: snap signal envelope (Env.); red line: Kernel Env.).

In the processed signal, as presented in Figure 2b, after normalizing the signals over 1 Pa within a unit time (2 ms: 192 samples) and taking the envelope, the median signal for all measurement periods was defined as the kernel function (κ). The normalized correlation coefficient between the kernel function (κ) and the signal (ε) was obtained by normalizing the signals of the unit time length (2 ms: 192 samples) and taking the envelope (upper envelope using a moving Hilbert filter with a length of about 10% (19 samples)) is called score, S (t), as shown in Equation (1). Snapping shrimp signals were identified and counted when a score value over 0.78 and a signal over 120 dB were satisfied. The score threshold of 0.78 is the top 1% of the total score during this period [16,17,29].

$$\textbf{Percent excess snap rate}(\%) = \frac{N_s - N_d}{N_d} \times 100 \quad (2)$$

The percent excess snap rate in Equation (2) represents the relative snap rate compared to the daytime. N_s is the number of snap rates of the signal, and N_d is the number (N_d: 2167 in 1st, 1819 in 2nd [min^{-1}]) of the minimum snap rate at daytime between sunrise and sunset.

2.3. Wavelet Transform Analysis

Tide has directional components, so the tidal level was normalized over the maximum amplitude to compare with the snap rate. The continuous wavelet analysis was performed to analyze the normalized tidal level and snap rate. The tidal level was continuously collected for 96 days. However, the snap rate data was missed for 6 days from 26 October to 31 October 2019 due to the battery changing of the hydrophone. Therefore, filling in this

missing snap rate data (6 days) for a long-term analysis was necessary. A circadian pattern was created by averaging 15 days (one cycle of moon phases) before and after the missing data. Then, the long-term pattern was added by the moving average value of 90 days (six cycles of the moon phases). A MATLAB function was employed for wavelet calculation with the wavelet type 'Morlet' [16,30–35]. This wavelet analysis provides a good balance between time and frequency localization.

3. Results

The circadian and tidal changes in the snap rate of snapping shrimp were analyzed using long-term acoustic data measured by a moored hydrophone. The long-term trends of the snap rate with water temperature and tidal level are plotted in Figure 3. It was confirmed that the mean snap rate decreased from 2500 to 2000 times per minute, and the water temperature decreased from 25 °C to 18 °C during the measurement period. It is concluded that the mean snap rate is directly proportional to the water temperature at 71 times per minute for every 1 °C change for 90 days from mid-September. On average, the tidal level decreased from 190 cm to 140 cm (snap rate change per tidal level: 10 times/min/cm), though it varied with moon phase changes between the new moon and full moon. The snap rate was found to be related to the mean tidal level and its high and low tide variations.

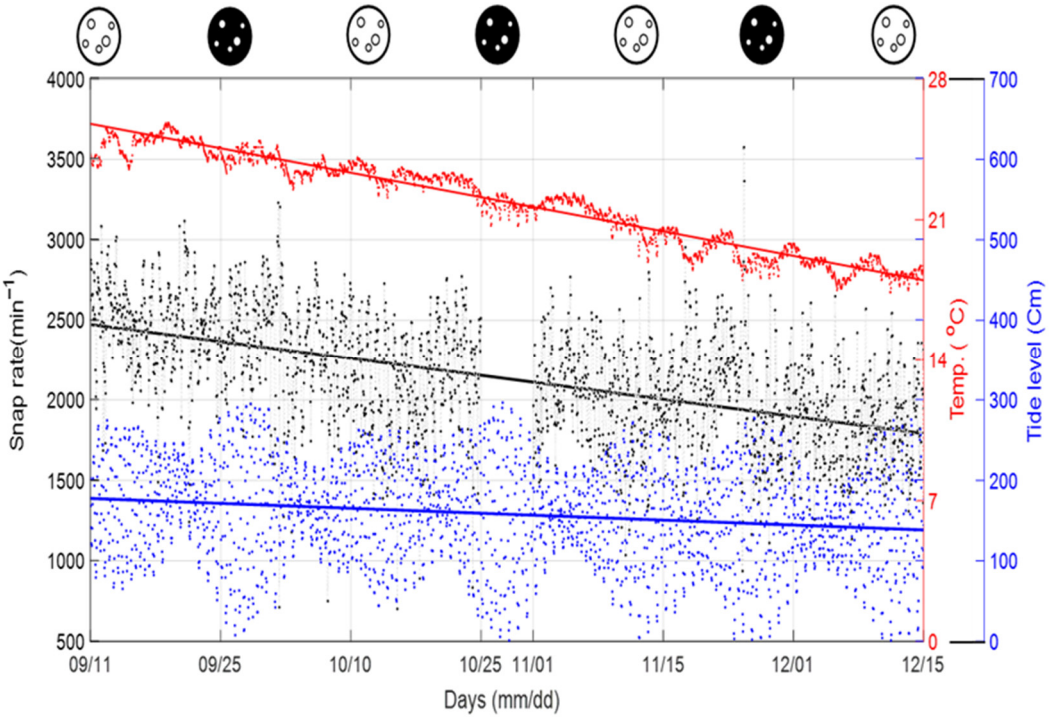


Figure 3. Long-term trends of snap rate (black dots; black line: linear fitting of snap rate), water temperature (red dots; red line: linear fitting of temperature), and tide level (blue dots; blue line: linear fitting of tide level). White and dark circles are the full moon and new moon, respectively.

3.1. Diurnal Pattern

There were some distinct patterns of snapping sounds during the measurement period, as shown in Figure 4a. First, a high snap rate at sunrise and sunset is indicated by arrowheads, and the pattern is evident in winter. Second, the overall snap rate decreases from September to December. Third, there is a higher and lower pattern of snap rate twice a day. The means and standard deviations of the snap rate for the first-half and the second-half periods were 2304 ± 442 and 1961 ± 435 per minute, respectively, as shown in Figure 4b. The snap rate decreased from the first to the second half, mainly due to reduced water temperature and mean tidal level. Snap rate per minute was averaged to 2435 and 1973 at

night and 2168 and 1902 during the day for the first- and second-half periods, respectively. At sunrise and sunset, the snap rate was much higher, up to 2355 in the second-half period, than during the day and night. In the first half, there was no sharp increase in the snap rate at sunrise and sunset; rather, a higher snap rate was observed at night. The percent excess snap rate is plotted in Figure 4c, and the mean snap rate increased up to 21% at night and 17% at sunrise and sunset compared with the one at daytime in the first-half period. However, the percent excess snap rate had a sharp peak at dawn at 24% and another small peak of 17% at sunset. The snap rate right after sunset decreased to 10% and then increased to 15% at midnight. Then, the snap rate was reduced to 3% just before sunrise in the second-half period. The percent excess snap rate difference between the first and second periods was the highest at night.

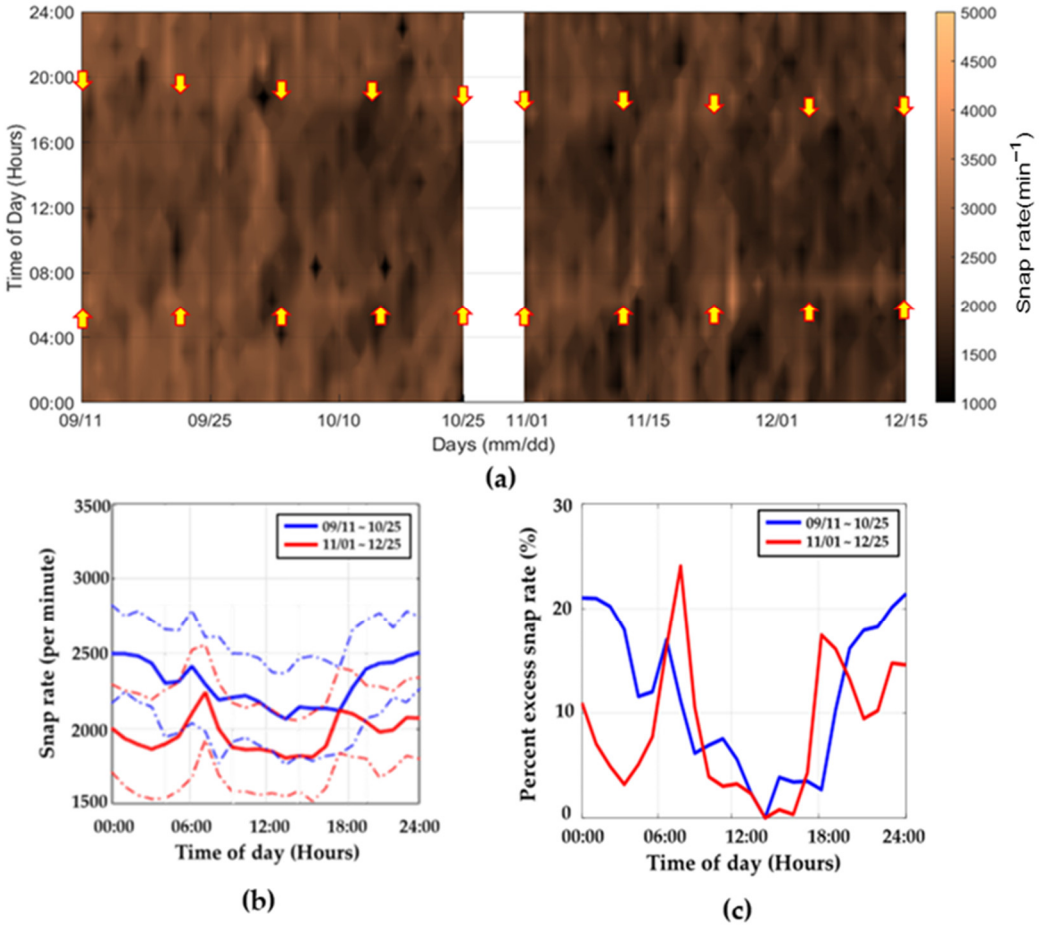


Figure 4. Circadian pattern of the snap rate of snapping shrimp. (**a**) Snap rate by day on the x-axis (9/11~12/15) and hour on the y-axis: (00:00~24:00). Color bar: snap rate per minute. Arrowheads are pointing to the sunrise and sunset times. (**b**) Mean and standard deviation of the snap rates in a day. (**c**) The percentage excess snap rate in a day.

3.2. Tidal Pattern

The snap rate pattern followed the tidal cycle and was higher at high tide and lower at low tide, as shown in Figure 5. The line plot of Figure 5a depicts the per-hour change in the snap rate for 90 days and the difference at low and high tides. The means and standard deviations of the snap rate at high tide were 2205 ± 320 and 1957 ± 372 in the first- and second-half periods, respectively, and those at low tides were 2100 ± 320 and 1800 ± 320 (Figure 5b). The mean snap rate was 13% higher at high tide ($p < 0.001$) than at low tide. As a result of period analysis using fast Fourier transforms, the solar and half-diurnal casting cycles were dominant. Tidal signals show strong semidiurnal and diurnal components

with some other components, such as four and six times a day. Based on this, the snap rate explains that the diurnal component is dominant, followed by the semi-diurnal component among the components of the tidal cycle (Figure 5c).

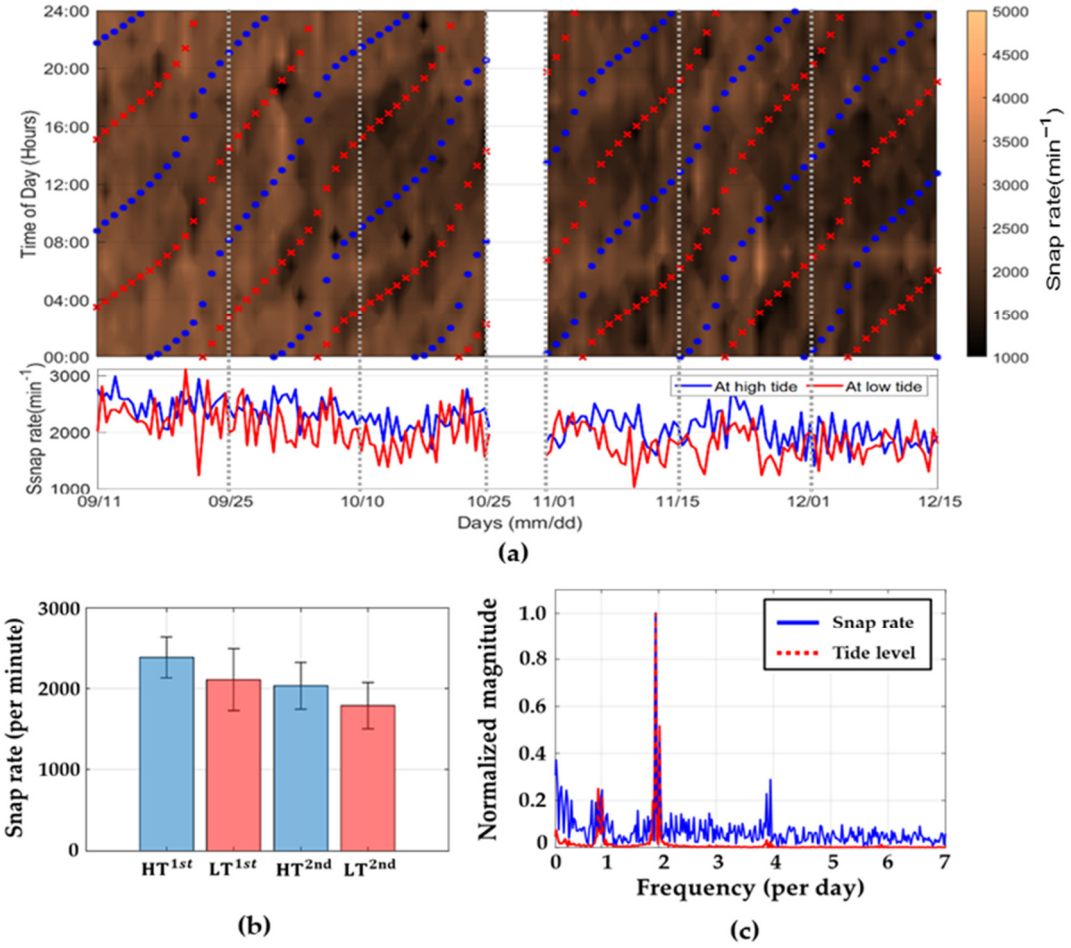


Figure 5. The tidal pattern of the snap rate of snapping shrimp. (**a**) Snap rate by day on the x-axis (9/11~12/15) and hour on the y-axis: (00:00~24:00). Color bar: snap rate per minute. The blue circles are the times of high tide, and the red marks of x represent the low tide. The snap rate was lower at low tide than at high tide. (**b**) Mean snap rates and standard deviations at high and low tides show significant differences at the 1st- and 2nd-half periods. (**c**) Fast Fourier transform (FFT) of snap rate and tidal level.

Figure 6 presents the wavelet analysis to show the coherence between the snap rate of snapping shrimp and the tidal level. They have a strong coherence with semidiurnal (0.5 day, K2 = 0.50) and diurnal (1 day, K1 = 1.00) periods. Therefore, the semidiurnal tide from the principal lunar and solar components and the diurnal tide from lunisolar and principal lunar periods affect the snap rate [31,36]. Longer periods, such as 15 days (lunar cycle: Mf = 13.65, Mm = 27.5), have relatively weak coherence because of the shorter period pattern.

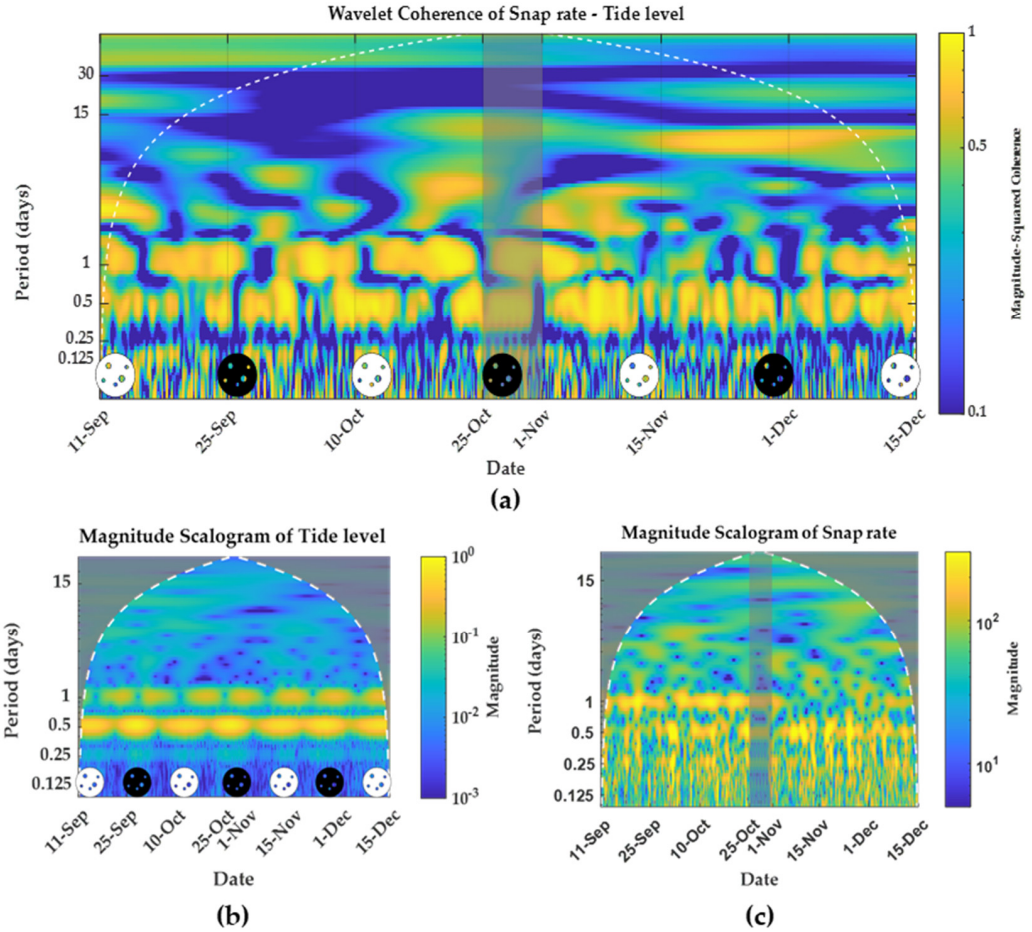


Figure 6. Wavelet transform analysis of snap and tide level. (○: Full moon, ●: New moon, ■: fill in the missing snap rate data); The wavelet analysis results in (**a**) coherence between snap rate and tidal level, (**b**) tidal level, and (**c**) snap rate.

4. Discussion

The long-term mooring measurements of ambient noise demonstrated a proportional relationship between the snap rate and the surface water temperature at 71 times/minute for every 1 °C. The fluctuation of the snap rate was highest in the summer at night, sunrise, and sunset and lowest during the day in the coastal sea of western Jeju Island for 90 days from mid-September. The snap rate had a weak coherence with the tidal level for about 15 and 30 days (Lunar cycles), but the 45-day consecutive measurements were not enough to make a concrete conclusion. These results show the indirect measurements of snapping shrimp activity, which is highly related to water temperature and tidal level with a semidiurnal and diurnal variation.

Even though we measured the ambient noise twice for 45 days, there was a gap of 6 days (for hydrophone-battery and SD-card replacement) between the two measurements, making it challenging to have a consecutive long-term analysis of the tidal period. The high-frequency component disappeared while processing the unmeasured data for 6 days using a moving average, but there was no significant effect on circadian and lunar cycle changes. To compensate for this, a plausible way is employed to give an artificial signal-based mean and standard deviation correlated with different temperatures and tidal levels. It is expected that a more accurate long-term analysis will be possible if the analysis method that can fill this measurement gap is further supplemented by future research.

The quantitative analysis of snapping sound has rarely been done in situ. There is a recent paper regarding the sound of the snapping shrimp measured in relatively deep waters of the southern part of Korea [29]. Unlike this study, the snap rate was quantitatively

expressed by analyzing the data measured for a short period at depths where visible light rarely enters. Although there is a seasonal difference in the measurement period in May, a snap rate of 200 to 1200 times occurred, and the snap rate changed according to the sea level [31].

The circadian change of the snap rate of snapping shrimp was observed in a few studies as shown in Table 1. For example, in St. John, located in the Caribbean Sea, USA, the snap rate of snapping shrimp increased rapidly at sunrise and sunset, but it was higher during the day than at night [29]. In contrast, in North Carolina (USA), day and night snap rates changed with measurement time [16]. Meanwhile, at the Ieodo Science Station in the south of Jeju, the snap rate of snapping shrimp showed a change with wind speed but did not exhibit a circadian pattern [15].

Table 1. Previous literature on snapping shrimp diurnal patterns.

Site (Duration)	Measurement Period (Days)	Sample Rate [kHz]	Snap Rate (min^{-1}) and Percent Excess Snap Rate (%)			Depth	Location	Ref.
			Day Time [N_d]	Night Time	Sunrise and Sunset			
Site 1 (1 min/10 min)	19/04/13~ 06/07/13 **(79 days)**	80	1000	800 (−20.0)	1220 (20.0)	12 m	Tektite, St. Jone, **USVI**	[29]
		80	1800	1600 (−11.0)	2250 (25.0)	10 m	Yawzi, St. Jone, **USVI**	
Site 2 (1 min/15 min)	19/09/11~ 26/09/11 **(7 days)**	50	1300	1070 (17.7)	1510 (16.2)	3 m	North Carolina, **USA**	[16]
	21/10/11~ 28/10/11 **(7 days)**	50	1100	720 (−34.5)	1180 (7.3)	3 m		
Site 3 (10 min/60 min)	11/09/19~ 25/10/19 **(45 days)**	192	2167	2435 (12.3)	2440 (12.5)	20 m	Jeju-si, Jeju, **South Korea**	Current study
	01/11/19 ~ 15/12/19 **(45 days)**	96	1819	1973 (3.7)	2355 (23.8)	20 m		

Ocean currents change due to tide, affecting underwater ambient noise's low-frequency band. In our previous study in the same sea area, there was a change in the tide in the low-frequency band below 100 Hz of the ambient noise [20]. In a previous study on the correlation between underwater noise and sea level at Ieodo, the underwater noise also changed according to the tidal change and the phase of the moon [37]. Although the study of prawns conducted in the same sea area did not show circadian characteristics, the snap rate of prawns changed according to the tidal change (Table 2) [31]. According to the soundscape for various fish species such as *Miichthys miiuy* (brown croaker) and *Lophius piscatorius* (angler), there was a noticeable change with the tide but not with the moon phase. Still, the tidal difference was insignificant in the case of snapping shrimp [17]. However, this study confirmed that the snap rate of snapping shrimp showed tidal variation and semidiurnal and diurnal changes.

Table 2. Previous literature on snapping shrimp tidal patterns.

Site (Duration)	Duration	Sample Rate	Snap Rate (Increase Rate,%)		Depth	Location	Ref.
			Low Tide	High Tide			
Site 1 (1 min/1 min)	20/05/15~ 25/05/15 **(5 days)**	100	620	780 (26)	100 m	Ieodo, Jeju, **South Korea**	[31]
Site 2 (10 min/60 min)	11/09/19~ 25/10/19 **(45 days)**	192	1957	2205 (12.7)	20 m	Jeju-si, Jeju, **South Korea**	Current study
	01/11/19~ 15/12/19 **(45 days)**	96	1800	2100 (16.6)	20 m		

5. Conclusions

In this study, acoustic data were collected through a hydrophone for 90 days from September to December 2019 on the western coast of Jeju Island in South Korea. The periodic characteristics of the snap rate of snapping shrimps were identified by the kernel signal's correlation coefficient and pressure threshold in the time-series signal. As a significant result, the circadian and lunar patterns of snapping shrimp were confirmed. First, we confirmed the daily cycle characteristics of the snap rate of snapping shrimp, a 17–24% increase compared to the daytime mean at sunrise and sunset and 10–21% higher at night during fall. Second, in the tidal cycle characteristics, the snap rate at high tide was 13% higher than that at low tide. The snap rates were also affected by semidiurnal and diurnal changes. During the entire measurement period, the water temperature decreased from 25 °C to 18 °C during the time of transition from September to December, and the snap rate also reduced from 2500 to 2000 times/minute. Therefore, the snap rate is changed to 71 times/minute per 1 °C for 90 days from mid-September. Although the water temperature and sea level showed a decreasing trend during the measurement period, the relationship may also change to seasons. It is necessary to explore the relationship between various environmental factors and the snap rate through long-term monitoring for a year or more.

Author Contributions: Conceptualization, I.J. and D.-G.P.; methodology, I.J. and D.-G.P.; software, I.J.; validation, I.J. and D.-G.P.; formal analysis, I.J.; investigation, I.J.; resources, D.-G.P.; data curation, I.J.; writing—original draft preparation, I.J.; writing—review and editing, I.J. and D.-G.P.; visualization, I.J.; supervision, D.-G.P.; project administration, D.-G.P.; funding acquisition, D.-G.P. All authors have read and agreed to the published version of the manuscript.

Funding: The Basic Science Research Program supported this research at the Research Institute for Basic Sciences (RIBS) of Jeju National University through the National Research Foundation of Korea (NRF), funded by the Ministry of Education. (2019R1A6A1A10072987) and the Government of Republic of Korea through a grant (MSIT, No.2018R1A2B2007997).

Institutional Review Board Statement: Not applicable.

Informed Consent Statement: Not applicable.

Data Availability Statement: The data supporting this study are available from the corresponding author upon reasonable request.

Acknowledgments: The authors appreciate the contributions of Hafiz Muhamad Umer Farooqi for proofreading and editing the manuscript.

Conflicts of Interest: The authors declare no conflict of interest.

References

1. Wenz, G.M. Acoustic Ambient Noise in the Ocean: Spectra and Sources. *J. Acoust. Soc. Am.* **1962**, *34*, 1936–1956. [CrossRef]
2. Urick, R.J. *Principles of Underwater Sound*; McGraw-Hill: New York, NY, USA, 1983; pp. 328–376.
3. Lurton, X. *An Introduction to Underwater Acoustics*; Springer: Berlin/Heidelberg, Germany, 2002; pp. 328–376.
4. Yang, T.; Yoo, K. Modeling the environmental influence on the vertical directionality of ambient noise in shallow water. *J. Acoust. Soc. Am.* **1997**, *101*, 2541–2554. [CrossRef]
5. Knobles, D.; Joshi, S.; Gaul, R.; Graber, H.; Williams, N. Analysis of wind-driven ambient noise in a shallow water environment with a sandy seabed. *J. Acoust. Soc. Am.* **2008**, *124*, EL157–EL162. [CrossRef]
6. Madsen, P.T.; Wahlberg, M.; Tougaard, J.; Lucke, K.; Tyack, P. Wind turbine underwater noise and marine mammals: Implications of current knowledge and data needs. *Mar. Ecol. Prog. Ser.* **2006**, *309*, 279–295. [CrossRef]
7. Vasconcelos, R.O.; Amorim, M.C.P.; Ladich, F. Effects of ship noise on the detectability of communication signals in the Lusitanian toadfish. *J. Exp. Biol.* **2007**, *210*, 2104–2112. [CrossRef] [PubMed]
8. Hildebrand, J.A. Anthropogenic and natural sources of ambient noise in the ocean. *Mar. Ecol. Prog. Ser.* **2009**, *395*, 5–20. [CrossRef]
9. Hermannsen, L.; Beedholm, K.; Tougaard, J.; Madsen, P.T. High frequency components of ship noise in shallow water with a discussion of implications for harbor porpoises (*Phocoena phocoena*). *J. Acoust. Soc. Am.* **2014**, *136*, 1640–1653. [CrossRef]
10. Dahl, P.H.; Miller, J.H.; Cato, D.H.; Andrew, R.K. Underwater ambient noise. *Acoust. Today* **2007**, *3*, 23–33. [CrossRef]
11. Rogers, P.H.; Cox, M. Underwater sound as a biological stimulus. In *Sensory Biology of Aquatic Animals*; Springer: New York, NY, USA, 1988; pp. 131–149.

12. Lillis, A.; Eggleston, D.B.; Bohnenstiehl, D. Estuarine soundscapes: Distinct acoustic characteristics of oyster reefs compared to soft-bottom habitats. *Mar. Ecol. Prog. Ser.* **2014**, *505*, 1–17. [CrossRef]
13. Butler, J.; Stanley, J.A.; Butler, M.J., IV. Underwater soundscapes in near-shore tropical habitats and the effects of environmental degradation and habitat restoration. *J. Exp. Mar. Biol. Ecol.* **2016**, *479*, 89–96. [CrossRef]
14. Cato, D.H.; Bell, M.J. *Ultrasonic Ambient Noise in Australian Shallow Waters at Frequencies up to 200 kHz*; Materials Research Labs Ascot Vale (Australia): Ascot Vale, Australia, 1992.
15. Jung, S.-K.; Choi, B.; Bong-Chae, K.; Kim, B.-N.; Kim, S.H.; Park, Y.; Lee, Y.-K. Seawater Temperature and Wind Speed Dependences and Diurnal Variation of Ambient Noise at the Snapping Shrimp Colony in Shallow Water of Southern Sea of Korea. *Jpn. J. Appl. Phys.* **2012**, *51*, 07GG09. [CrossRef]
16. Bohnenstiehl, D.; Lillis, A.; Eggleston, D. The Curious Acoustic Behavior of Estuarine Snapping Shrimp: Temporal Patterns of Snapping Shrimp Sound in Sub-Tidal Oyster Reef Habitat. *PLoS ONE* **2016**, *11*, e0143691. [CrossRef]
17. Ricci, S.; Eggleston, D.B.; Bohnenstiehl, D.; Lillis, A. Temporal soundscape patterns and processes in an estuarine reserve. *Mar. Ecol. Prog. Ser.* **2016**, *550*, 25–38. [CrossRef]
18. Radford, C.A.; Jeffs, A.G.; Tindle, C.T.; Montgomery, J.C. Temporal patterns in ambient noise of biological origin from a shallow water temperate reef. *Oecologia* **2008**, *156*, 921–929. [CrossRef]
19. Staaterman, E.; Paris, C.B.; DeFerrari, H.A.; Mann, D.A.; Rice, A.N.; D'Alessandro, E.K. Celestial patterns in marine soundscapes. *Mar. Ecol. Prog. Ser.* **2014**, *508*, 17–32. [CrossRef]
20. Jeong, I.; Min, S.; Paeng, D.-G. Moored measurement of the ambient noise and analysis with environmental factors in the coastal sea of Jeju Island. *J. Acoust. Soc. Korea* **2020**, *39*, 390–399.
21. Au, W.W.; Banks, K. The acoustics of the snapping shrimp Synalpheus parneomeris in Kaneohe Bay. *J. Acoust. Soc. Am.* **1998**, *103*, 41–47. [CrossRef]
22. Versluis, M.; Schmitz, B.; Von der Heydt, A.; Lohse, D. How snapping shrimp snap: Through cavitating bubbles. *Science* **2000**, *289*, 2114–2117. [CrossRef]
23. Kim, B.-N.; Hahn, J.; Choi, B.; Bong-Chae, K. Snapping Shrimp Sound Measured Under Laboratory Conditions. *Jpn. J. Appl. Phys.* **2010**, *49*, 07HG04. [CrossRef]
24. Lohse, D.; Schmitz, B.; Versluis, M. Snapping shrimp make flashing bubbles. *Nature* **2001**, *413*, 477–478. [CrossRef]
25. Lillis, A.; Mooney, A. Loudly heard, little seen, and rarely understood: Spatiotemporal variation and environmental drivers of sound production by snapping shrimp. *Proc. Meet. Acoust. Acoust. Soc. Am.* **2016**, *27*, 010017. [CrossRef]
26. Bibikov, N.G.; Serebryany, A.N.; Ivanov, M.P.; Ovchinnikov, O.B. *Snapping Shrimps Sound in Black Sea*; Universitätsbibliothek der RWTH Aachen: Aachen, Germany, 2019.
27. Zhang, X.; Ying, W.; Yang, P.; Sun, M. Parameter estimation of underwater impulsive noise with the Class B model. *IET Radar Sonar Navig.* **2020**, *14*, 1055–1060. [CrossRef]
28. Mahmood, A.; Chitre, M. Modeling colored impulsive noise by Markov chains and alpha-stable processes. In Proceedings of the OCEANS 2015-Genova, Genova, Italy, 18–21 May 2015; pp. 1–7.
29. Lillis, A.; Mooney, T.A. Snapping shrimp sound production patterns on Caribbean coral reefs: Relationships with celestial cycles and environmental variables. *Coral Reefs* **2018**, *37*, 597–607. [CrossRef]
30. Grinsted, A.; Moore, J.C.; Jevrejeva, S. Application of the cross wavelet transform and wavelet coherence to geophysical time series. *Nonlinear Process. Geophys.* **2004**, *11*, 561–566. [CrossRef]
31. Lee, D.H.; Choi, J.W.; Shin, S.; Song, H. Temporal Variability in Acoustic Behavior of Snapping Shrimp in the East China Sea and Its Correlation with Ocean Environments. In *Innovation and Discoveries in Marine Soundscape Research*; Frontiers Media SA: Lausanne, Switzerland, 2022.
32. Salih, A.R.C.; Farooqi, H.M.U.; Kim, Y.S.; Lee, S.H.; Choi, K.H. Impact of serum concentration in cell culture media on tight junction proteins within a multiorgan microphysiological system. *Microelectron. Eng.* **2020**, *232*, 111405. [CrossRef]
33. Farooqi, H.M.U.; Kang, B.; Khalid, M.A.U.; Salih, A.R.C.; Hyun, K.; Park, S.H.; Huh, D.; Choi, K.H. Real-time monitoring of liver fibrosis through embedded sensors in a microphysiological system. *Nano Converg.* **2021**, *8*, 3. [CrossRef]
34. Chethikkattuveli Salih, A.R.; Hyun, K.; Asif, A.; Soomro, A.M.; Farooqi, H.M.U.; Kim, Y.S.; Kim, K.H.; Lee, J.W.; Huh, D.; Choi, K.H. Extracellular Matrix Optimization for Enhanced Physiological Relevance in Hepatic Tissue-Chips. *Polymers* **2021**, *13*, 3016. [CrossRef]
35. Farooqi, H.M.U.; Khalid, M.A.U.; Kim, K.H.; Lee, S.R.; Choi, K.H. Real-time physiological sensor-based liver-on-chip device for monitoring drug toxicity. *J. Micromech. Microeng.* **2020**, *30*, 115013. [CrossRef]
36. Ollivier, B.; Shute, P.; Kinda, G.B. Underwater soundscape description from cyclostationarity point of view. *J. Acoust. Soc. Am.* **2021**, *150*, 2245–2255. [CrossRef]
37. Kim, S.H.; Choi, B.K.; Kim, B.-N. Correlation between Underwater Noise and Sea Level at Ieodo Ocean Research Station. *J. Mar. Sci. Eng.* **2021**, *9*, 1. [CrossRef]